

Does cefuroxime alter fracture healing in vivo? A micro computertomographic, biomechanical, and histomorphometric evaluation using a rat fracture model

Oliver Bissinger, Kilian Kreutzer, Klaus Dietrich Wolff, Gabriele Wexel, Alexander Hapfelmeier, Christoph Pautke, Stephan Vogt, Peter Michael Proding, Thomas Tischer

Angaben zur Veröffentlichung / Publication details:

Bissinger, Oliver, Kilian Kreutzer, Klaus Dietrich Wolff, Gabriele Wexel, Alexander Hapfelmeier, Christoph Pautke, Stephan Vogt, Peter Michael Proding, and Thomas Tischer. 2017. "Does cefuroxime alter fracture healing in vivo? A micro computertomographic, biomechanical, and histomorphometric evaluation using a rat fracture model." *Journal of Biomedical Materials Research Part B: Applied Biomaterials* 105 (8): 2282–91. <https://doi.org/10.1002/jbm.b.33759>.

Does cefuroxime alter fracture healing *in vivo*? A micro-computertomographic, biomechanical, and histomorphometric evaluation using a rat fracture model

Oliver Bissinger,¹ Kilian Kreutzer,¹ Klaus-Dietrich Wolff,¹ Gabriele Wexel,² Alexander Hapfelmeier,³ Christoph Pautke,¹ Stephan Vogt,^{2,4} Peter Michael Prodinger,² Thomas Tischer^{2,5}

¹Department of Oral and Maxillofacial Surgery, Klinikum rechts der Isar der Technischen Universität München, 81675 Munich, Germany

²Department of Orthopaedic Sports Medicine, Klinikum rechts der Isar der Technischen Universität München, 81675 Munich, Germany

³Institute of Medical Statistics and Epidemiology, Klinikum rechts der Isar der Technischen Universität München, 81675 Munich, Germany

⁴Department of Orthopaedic Sports Medicine, Hessing Stiftung Augsburg, Augsburg, Germany

⁵Department of Orthopaedic Surgery, Universitymedicine Rostock, 18057 Rostock, Germany

INTRODUCTION

Fracture healing is a dynamic process of bone remodeling and its understanding is essential for achieving optimal outcomes in clinical practice. The influence of some drugs on fracture healing is well known, whereas other therapeutics are less well investigated.^{1,2}

Antibiotics are frequently used for the prophylaxis and treatment of pre- and postoperative infections in bone surgery. However, the influence of most antibiotics on

bone healing is not studied sufficiently.³ Cefuroxime is a second generation cephalosporin with a broad antimicrobial activity not only against Gram-positive bacteria, namely staphylococcal and streptococcal strains, but also against Gram-negative organisms. It exhibits adequate bone penetration and is effective against most of the bacterias causing deep infection.⁴ Thus, cefuroxime is one of the most commonly used antibiotics for perioperative prophylaxis in bone surgery.⁵

Correspondence to: Dr. O. Bissinger; e-mail: oliver.bissinger@tum.de

Contract grant sponsor: Kommission für Klinische Forschung (Technische Universität München), KKF; contract grant number: C78-08

Other applications include bone cement impregnated with antibiotics in cases of total joint replacement or septic bone surgery.^{6,7} Because drug release from the cement is continuous, the use of antibiotic-impregnated bone cement for prophylaxis may also lead to a prolonged antibiotic effect on bone cells.⁸

However, recent *in vitro* studies have revealed inhibiting and toxic effects of high concentrations of antibiotics on osteoblasts *in vitro*^{9,10} and, in particular, Salzmann et al. showed that higher doses of cefuroxime significantly impaired the proliferation, differentiation and metabolism of osteoblasts *in vitro*.⁵

As bone remodeling demands the coordination of various cell types and the activation of diverse specific signaling pathways, cell culture might not be sufficient to imitate the whole process that finally results in the restoration of bone.¹¹ Since cefuroxime is widely used, a detailed evaluation of its *in vivo* effects on fracture healing would be of great importance for clinical practice, since such an examination has not as yet been carried out so far to the best of our knowledge. We have therefore evaluated the use of cefuroxime in a standardized closed femur fracture model to examine the following questions: (1) Does cefuroxime treatment alter biomechanical parameters assessed by three-point bending? (2) does cefuroxime alter quantitative μ CT parameters of the callus? (3) does cefuroxime alter histological morphology in terms of the composition of the callus?

MATERIALS AND METHODS

Animal model

All animal procedures were approved by the local animal research committee, in accordance with German legislative requirements, and were performed at the Institute of Experimental Oncology and Therapy Research, Centre for Preclinical Research at the Technical University of Munich (reference number of Regierung von Oberbayern: 55.2-1-54-2531-15-08).

Male 16-week-old adult Wistar rats (CRL: WI, mean weight \pm SD: 500 g \pm 50 g) were obtained from Charles River Laboratories (Sulzfeld, Germany). According to the standards for animal care, the rats were housed in open cages (polysulfone type III OTC), with a base area of 825 cm² (Ehret, Emmendingen, Germany) at 23–25°C (humidity (55 \pm 5%)) under a 12-h light/dark cycle and allowed free access to water and standard laboratory pellets. After acclimatisation for at least 2 weeks, animals were randomized and allocated to the different arms (Cefuroxime or Control) and groups (Group A: histology and μ CT, 6 animals per group; Group B: biomechanical Testing, 11 animals for cefuroxime and 11 animals for control) of the study (Table I).

Surgery

Preoperatively, the rats were anesthetized with Medetomidine (Medetomin, 0.15 mg/kg, Dechra Veterinary Products, 's-Hertogenbosch, Netherlands), Midazolam (Midazolam, 2 mg/kg, Hexal AG, Germany) and Fentanyl (Fentadon, 5

TABLE I. Study Setup Indicating the Corresponding Numbers of Specimens/Group for Analysis (After Exclusions)

Group	Cefuroxime	Control
A: Histology/ μ CT	6x	6x
B: Biomechanics	9x	11x

Group A: Histology and μ CT; Group B: Biomechanical testing.

μ g/kg, Dechra Veterinary Products) via intramuscular (i.m.) injection.

After preparing the approach to the intertrochanteric fossa the femoral neck was grasped with a curved forceps and a 1.0 mm K-wire was drilled into the intramedullary cavity [Figure 1(A)]. Distally, the pin reached the supracondylar region without perforating the cortical bone, so as not to interfere with knee function. After a radiographic control in 2 planes via C-arm (Siemens, Erlangen, Germany), the pin was cut flush with the cortex. A standardized fracture at the middle of the diaphysis of the pinned femur was accomplished by a specially designed blunt guillotine as described previously by Bonnarens et al.¹² This consisted of a 500 g weight (fall height: 35 cm) driving a blunt guillotine downwards (travel distance: 3 mm) onto an outstretched leg placed across an open platform, thereby creating a 3-point bending mechanism [Figure 1(B)]. Following this procedure, plain X-rays controls were obtained for position control [Figure 1(C)].

At the end of the operation, an antidote combination was given subcutaneously (s.c.), composed of Atipamezole (Antisedan, 0.75 mg/kg, Orion Corporation, Espoo, Finland), Flumazenil (Flumazenil, 0.2 mg/kg, Hexal AG) and Naloxone hydrochloride (Naloxone, 0.12 mg/kg, Braun AG, Germany) to end the anesthesia. During the postoperative period, pain was relieved by subcutaneous administration of buprenorphine twice a day (Buprenodale, 0.05 mg/kg, Dechra Veterinary Products). Postoperatively, no immobilization of the operated limb was necessary. The animals were able to load the leg immediately.

Cefuroxime (Cefuroxim Fresenius, Fresenius Kabi AG; 30 mg/kg BW) was administered daily. Control animals received a sodium chloride solution subcutaneously. On day 5 of the experimental setup, blood samples were taken from the venous angle of all animals under anesthesia with isoflurane to check the serum levels of cefuroxime (2–3 h after administration).

Before the rats were sacrificed on day 21 by an overdose of Narcoren (sodium pentobarbital, 400 mg/kg BW), they were anesthetized in plastic chambers by inhalation of isoflurane and blood was taken once more to determine the serum levels of cefuroxime (via puncture of the heart). After being harvested, all femora were freed of soft tissue [Figure 1(D)].

According to the group allocation, the bones were fixed in 100% methanol (histology/ μ CT) and stored at 4°C or were fresh-frozen and stored at –20°C (biomechanical group). Analyses were carried out after removal of the pin, either via biomechanical testing or μ CT. All evaluations were performed by blinded researchers.

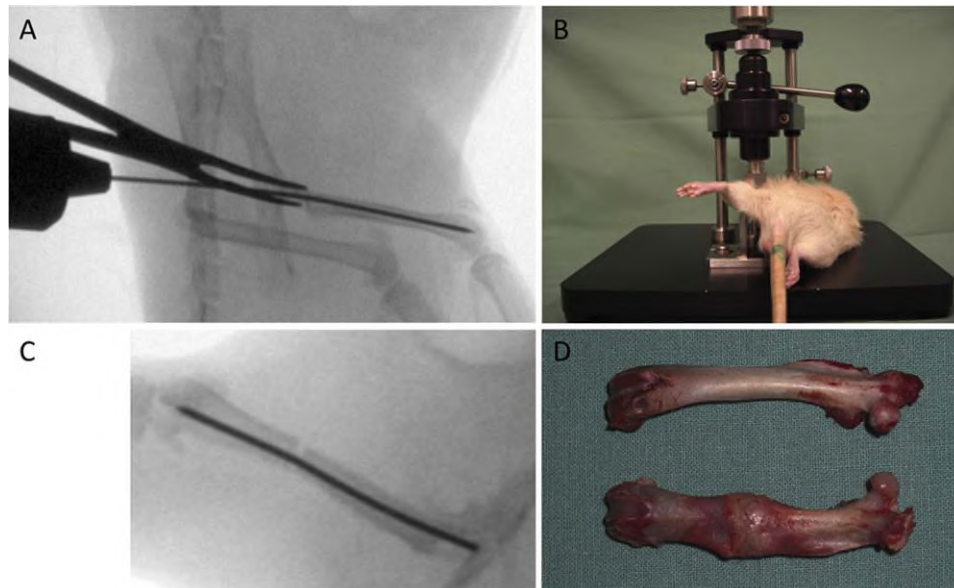


FIGURE 1. Surgical procedure and harvesting: A: C-arm control after insertion of the Kirschner-wire into the intramedullary cavity. Femoral neck grasped with the forceps. B: Femur placed on a blunt guillotine to produce a closed transverse fracture. (C) Postoperative C-arm control and (D) macroscopical control after 21 days.

Micro CT

Initially, a scout view was done and after determination of the scanning area [Figure 2(A)], specimens were scanned (~1 h) in methanol by using an isotropic voxel size of 10 μm (55 kVp, 145 μA ; μCT 40, Scanco Medical, Brüttisellen, Switzerland). The integration time was set at 200 ms. For each sample exactly 620 micro-tomographic slices with a slice increment of 10 μm were acquired covering both sides of the fracture gap (each 3,1 mm).¹³ Because of the beam hardening effects, a correction algorithm was applied based on a 1200 mg hydroxyapatite (HA)/ cm^3 phantom, which is thought to be superior to the previously used 200 mg HA/ cm^3 phantom.¹⁴

Differences in the brightness of the pixels were evident [Figure 2(B,C)], so that thresholds could be determined visually by two independent examiners (based on all numbers of samples and histograms) to distinguish callus from original cortical bone, marrow, and solution.¹⁵ A constrained three-dimensional (3D) Gaussian filter was used to suppress the noise partly in the volumes. All samples were binarised by using the same parameters for callus [sigma (0.8), support (1) and threshold (150)] and original cortical bone [sigma (1.5), support (3), and threshold (370)]. A standard convolution-backprojection procedure with a Shepp and Logan filter was employed to reconstruct 3D CT images [Figure 2(D-H)].

Bone volume (BV, mm^3), tissue mineral density (TMD, $\text{mg HA}/\text{cm}^3$) and bone mineral content (BMC, defined as the callus BV multiplied by TMD, mg)^{14,16} as well as structure model index (SMI, dimensionless), degree of anisotropy (DA, dimensionless), bone surface (BS, mm^3), and trabecular thickness (Tb. Th., mm) as structural parameters (non-volume-depending parameters) were calculated.

Scans of a HA phantom provided by the system manufacturer for density calibration were performed previous to

this study to enable the calculation of TMD and BMC. To calculate TMD, two-voxel “peeling” was additionally applied to minimize partial volume effects.^{13,17}

Histological analysis

Following μCT analysis, the specimens were dehydrated in a graded series of ethanol (from 70% to 100% [v/v]) and acetone and were then embedded in methyl methacrylate (MMA). Subsequently, coronal sections of the MMA-embedded samples of $100 \pm 20 \mu\text{m}$ in thickness were made by using a sawing microtome (Leica, Wetzlar, Germany) technique. Selected specimens were additionally ground (70 μm) and polished (Schleifsystem 400 CS, Exakt, Germany). Laczkó and Lévai (LL) staining was applied for histological analysis. Overview images were performed with a Wild@ Macroscope M3Z (Wild, Heerbrugg, Switzerland) in motion function and analysis was carried out via bright-field microscopy (Axiophot 2; Zeiss, Jena, Germany). Detailed images were digitized with a Nikon Eclipse 50i microscope (Nikon, Düsseldorf, Germany) and a AxioCam Hrc video camera (Zeiss, Jena, Germany, magnification 10x). Semi-quantitative analysis was performed by using the image analysis system Axiovision 4.8 (Zeiss, Jena, Germany), modified from Hou et al. and Krischak et al.^{18,19} The two central sections were used to evaluate semi-quantitatively whether cartilage, connective tissue or newly formed bone was present in the area of the fracture gap. This was expressed as the percentage (%) of the samples with cartilage, connective tissue or bony callus in the area of the fracture gap. Furthermore, we investigated whether bony bridging of the fracture gap occurred or not. This was expressed as the percentage (%) of the samples with bony bridging of the fracture gap. The entire width of the gap did not have to be bridged with the osseous callus, since this was not expected

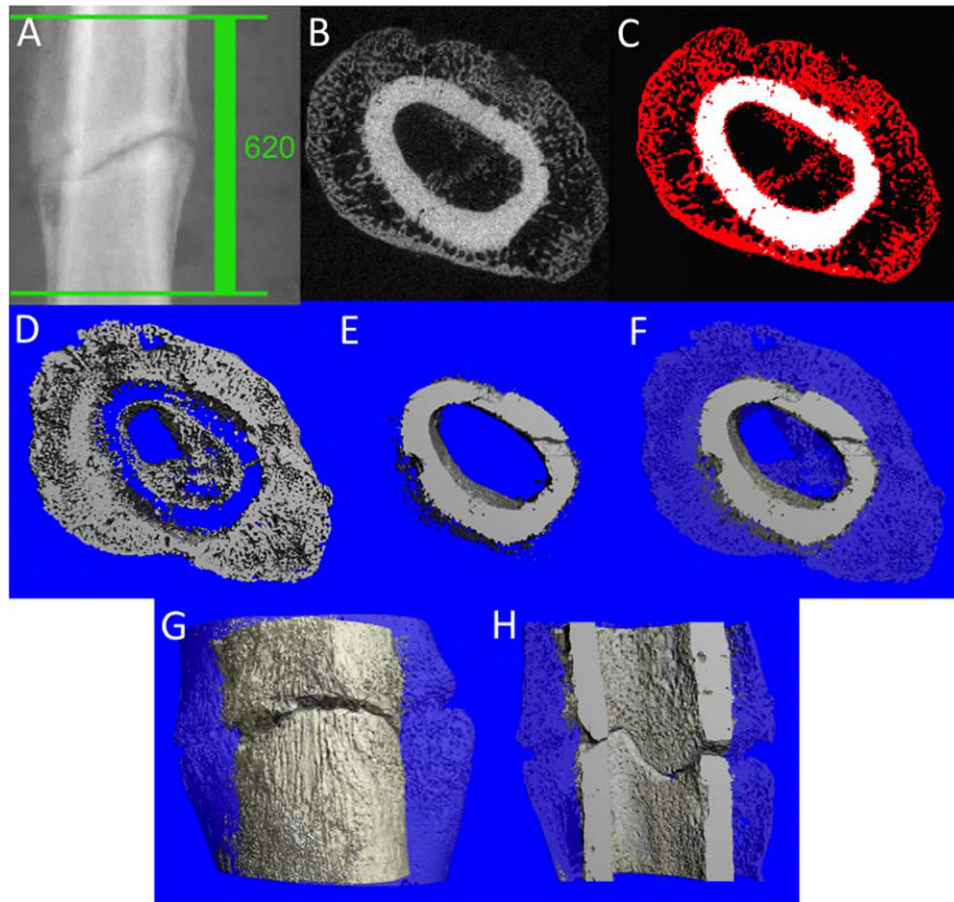


FIGURE 2. Scout view and determination of the scanning area within two reference lines (A). 2D axial μ Ct (B) gray value image of original cortical bone, callus and air/bone marrow and (C) corresponding fully automatic segmented image (callus = red); 3D axial μ CT reconstructions (Two Thresholding Procedure): (D) Peri- and endosteal callus, (E) cortical bone and (F) callus (blue and semitransparent) and cortical bone (gray). 3D coronar μ CT as an overview image (G) and half-sliced (H). All images represent the same specimen.

after 21 days. Staining distinguished bone tissue, which was stained red, from cartilage (blue) and fibrous connective tissue (pale blue to gray/white). New bone and new cartilage exhibited more intense staining.

Biomechanical testing

Femora were immediately tested after being thawed and were kept moist during the tests. Biomechanical examination of the specimens was performed by three-point bending on a Wolpert TZZ 707/386 material testing machine (Istron Wolpert GmbH, Darmstadt, Germany). According to Turner et al. the distance between the bearing- and loading-bars for each rat femur was 15 mm for 3-point bending with force transmission at the middle position between the distal and the proximal site of each femur.²⁰ The femora were placed on their posterior surface on the lower supports of the bending apparatus.²¹

The bending load was applied by a round-ended indenter with a persistent test velocity of 5 mm/min until failure (breaking load). As a termination criterion, a reduction in the force of > 50 N was defined. The failure criterion was a reduction in force of 80%. Failure load (N) and stiffness (N/

mm) were determined from the load-displacement diagram. The stiffness was deduced from the gradient of the linear part of the curve. The measurement data were collected by using the Test&Motion test program (DOLI Elektronik GmbH, Munich, Germany).

Statistical analysis

A power analysis was used to determine the number of animals.²² By allocating at least 9 animals per group, recognition of expected treatment effects of 14.5% would be feasible with a statistical power of 90% at a significance level of $\alpha = 0.05$ in the femur shaft three-point bending test assuming a standard deviation of 13.4%. Regarding μ CT and histology, a minimal sample size of 6 animals was chosen for exploratory investigations and the computation of descriptive statistics with no need for a power calculation. Statistical analysis was performed by using R 2.15.1 (The R Foundation for Statistical Computing, Vienna, Austria) and GraphPad Prism Version 4.00 (GraphPad Prism Software® San Diego, USA). Differences between the treatment groups were evaluated by unpaired two-sided Student's *t*-tests. All tests were conducted on exploratory 5% significance levels.

TABLE II. μ CT Parameters Within the VOI

		Mean \pm SD		Mean difference (95%-CI)	<i>p</i> values
BV	C	55.35 \pm 6.74	C vs K	-11.84 (-27.64-3.97)	0.120
	K	67.19 \pm 14.90			
TMD	C	647.87 \pm 13.01	C vs K	12.38 (-5.59-30.35)	0.155
	K	635.48 \pm 14.81			
BMC	C	35.84 \pm 4.20	C vs K	-6.70 (-15.88-2.48)	0.129
	K	42.54 \pm 8.61			
SMI	C	-0.24 \pm 0.46	C vs K	1.06 (0.26-1.86)	0.969
	K	-0.22 \pm 1.01			
DA	C	1.17 \pm 0.04	C vs K	-0.01 (-0.07-0.05)	0.743
	K	1.18 \pm 0.05			
BS	C	1369.01 \pm 163.86	C vs K	-267.82 (-630.86-95.21)	0.125
	K	1636.83 \pm 340.78			
Tb. Th.	C	0.095 \pm 0.004	C vs K	-0.003 (-0.007-0.001)	0.116
	K	0.098 \pm 0.003			

There were no relevant differences between cefuroxime and control.

The distribution of quantitative data is presented as mean values \pm standard deviation (mean \pm SD).

RESULTS

Inclusions and exclusions

A total of 32 out of 42 animals were included in the study. No infection, weight loss \geq 5% or severe swelling was observed. Ten animals (24%) had to be excluded because of complications related to the fracture model (no fracture, comminuted fracture or wrong site of the fracture).

Cefuroxime blood levels

Cefuroxime blood levels were detectable within the target range (2-20 μ g/mL; Medizinisches Versorgungszentrum Dr. Eberhard & Partner; Dortmund; first blood withdrawal: 3.07 μ g/mL; second blood withdrawal: 5.65 μ g/mL, average values).

μ CT

No relevant difference regarding bone volume (=absolute callus volume (peri- and endosteal) minus original cortical bone, surrounding air, and soft tissue) could be seen between the cefuroxime and the control group. The control group showed a wider spread of the values, which influenced the mean and SD (55.35 \pm 6.74 vs. 67.19 \pm 14.90, *p* = 0.120) [Table II and Figure 3(A)]. TMD (as a surrogate parameter for the stability and thus the quality of the newly formed bone) revealed, with respect to cefuroxime and the control, very homogeneous groups with only marginal differences [647.87 \pm 13.01 vs. 635.48 \pm 14.81, *p* = 0.155, Table II and Figure 3(B)]. BMC, which is calculated as density \times volume, had analogous tendencies in values to those for BV [Table II and Figure 3(C)].

Structural parameters are used to describe uniformly and to quantify the microarchitecture of examined objects (Table II). In general no relevant difference in structural parameters was observed between the two groups.

SMI as a dimensionless parameter describes the structure of the trabeculae independently of bone mineral density and trabecular thickness. Almost identical mean values

were generated between the cefuroxime and the control group (*p* = 0.969). The cefuroxime group again showed a smaller SD, whereas on the other hand, the control group had a higher SD because of two considerably high and low values [Table II and Figure 3(D)]. DA as a dimensionless pure 3D parameter describes the predominant spatial orientation of the trabeculae within the bone. Both groups were homogeneous with respect to the mean and SD without relevant differences (*p* = 0.743). The cefuroxime group contained an upward outlier [Table II and Figure 3(E)]. Bone surface (BS) in mm³ reflects the independent bone surface. With regard to the trend, the values were similar to BV (*p* = 0.125), [Table II and Figure 3(F)]. Tb. Th. represents the local bone (-trabecular) thickness in mm. The mean in the control group was slightly higher than that of the cefuroxime group (*p* = 0.116) [Table II and Figure 3(G)].

Histological analysis

In the control group, osteochondral bone union, and active new bone formations were determined indicating endochondral ossification [Figure 4(A,D,G)]. The cefuroxim group showed bony callus in the area of the fracture gap, analogous to that in the control group, in 67% of the samples [Figure 4(B)]. Furthermore, we investigated cartilage and fibrous connective tissue. Hyaline cartilage was mostly located perpendicular to the original cortical bone in the area of the gap [Figure 4(A,D)]. Calcified cartilage was evident in the transition zone from the cartilage to the woven bone (4E and H). In the cefuroxime group, the least cartilage was seen. In the control group, relatively more cartilage than bone was detected [Figure 4(B) left diagram]. Connective tissue as poor-quality tissue was detectable equally rarely within the fracture gap, both in the control and the cephalosporin group (33%). With regard to bony fracture gap bridging, the cefuroxime group was slightly more successful (50%) than the control group (33%) [Figure 4(B) right diagram]. Nevertheless, between the original cortical bone, mostly cartilage was detectable [Figure 4(E)]. A sample from the cefuroxime group [Figure 4(C,F,I)] revealed trabecular bone structure in the area that was formerly occupied

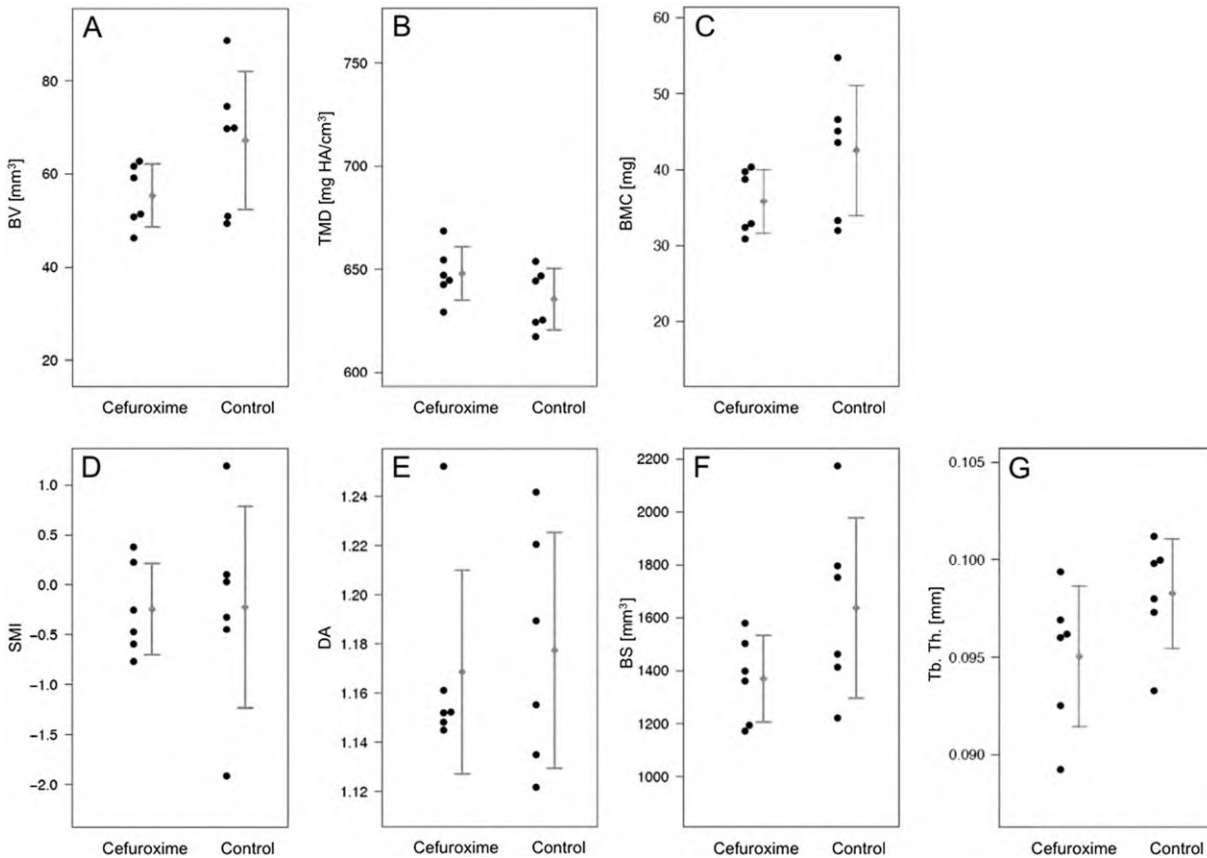


FIGURE 3. μ CT parameters as means \pm SD and dotplot of (A) BV, (B) TMD, (C) BMC, (D) SMI, (E) DA, (F) BS, and (G) Tb. Th. Mean differences and significances are shown in Table II.

by cartilage, a finding that was more often seen in the cefuroxime group than in the control group.

Biomechanics

In all femurs both the breaking load (maximum strength exerted on the bone) and the stiffness (regression of the curve of the load-displacement diagram) could be calculated.

No difference in the maximum failure load between the controls ($77.65 \pm 41.82 \text{ N}$) and cefuroxime ($78.54 \pm 20.52 \text{ N}$) was detected [$p = 0.95$, Table III, Figure 5(A)].

With regard to the stiffness, almost identical mean values ($p = 0.97$) were generated between the controls and cefuroxime. In detail, the values obtained from the experimental bones were $122.44 \pm 81.16 \text{ N/mm}$ for controls and $123.74 \pm 60.08 \text{ N/mm}$ for cefuroxime [Table III, Figure 5(B)].

DISCUSSION

Bone remodeling is a complex process that can be influenced by different drugs. Cefuroxime is an antibiotic widely used in patients receiving surgical fracture treatment, but has been shown to provoke a possible adverse effect on osteoblast function in cell culture experiments.⁵ Thus, a negative effect on bone remodeling *in vivo* was feasible, and should be further investigated.

In our study, cefuroxime administration over a period of three weeks during the process of fracture healing showed no adverse effects on fracture healing compared with the control group. Thus, the inhibition observed *in vitro* at high concentrations could not be confirmed in the animal model.

Salzmann et al. showed that higher doses of cefuroxime greatly impaired the proliferation, differentiation and metabolism of osteoblasts *in vitro*. This was most pronounced after 72 h (the longest observation period). These side effects seemed to be at least partially reversible. Lower concentrations, however, increased the proliferation, metabolism and calcium deposition of the cells.⁵ Since this medication is often used, the study of its detailed effect *in vivo* was of great importance for clinical practice.

Drugs in rats act in a similar way to those in human bone, because cells with similar receptors to those of bone cells in humans, e.g., osteoblasts and osteoclasts, were detected in rats. Therefore, preclinical animal rat models have a high prognostic value related to drug efficacy and safety in humans.¹¹ However, findings in animal fracture healing studies cannot be extrapolated directly to humans because of permanently open growth plates at the epiphyses of long bones and an absent Haversian system in rodents.¹¹ Long bones such as the femur and tibia are equally suitable for fracture healing studies. Because of the thin soft tissues surrounding the tibia, this is suitable as an

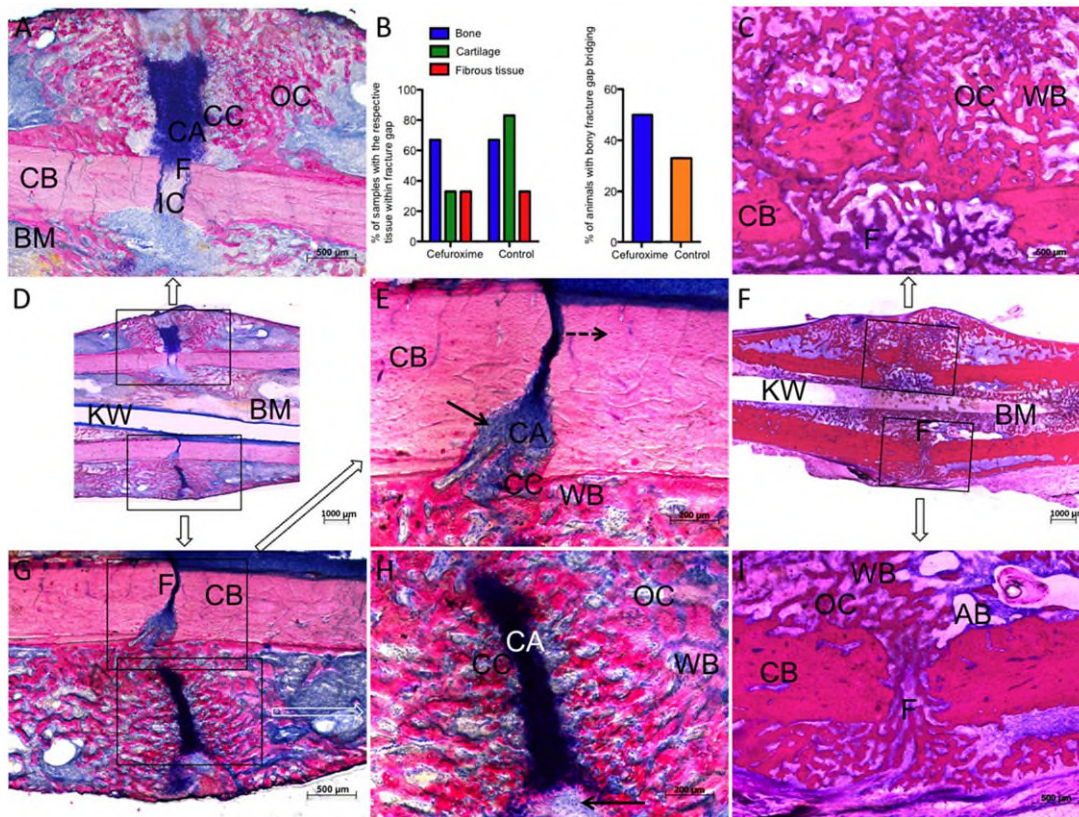


FIGURE 4. Representative histological images of fracture sites of the control (left and middle column: A, D, E, G, and H) and cefuroxime group (right column: C, F, and I). D and F: overview (10x), A and G as well as C and I: details of the respective area (40x). E and H: higher magnification (100x) images of the insets in G. In the control group, osteochondral bone union and active new bone formations were determined and even the outer periosteal OC bridged the gap (A, D, and G). Proximally and distally within the callus, air and lacunae of fibrous connective tissue were seen (A). CC was obvious indicating endochondral ossification. In the area between CB, cartilage was mostly detectable (E). Parallel-arranged osteocytes were seen in the area of CB and chondrocytes within the CA. The periosteal callus was divided into an inner shell that had grown over the original cortex and an outer shell that had encapsulated the callus and formed the new interface with the periosteum. In between (in the area of the gap), an area of hyaline CA ran perpendicular to the CB (G and H). In the transition zone from CA to WB, CC was evident (E and H). In C, F, and I, the space that was occupied by CA is replaced by trabecular bone structure. This occurred more often in the cefuroxime group (B) than in the control group. Fatty BM was replaced by bone. The area of the Kirschner wire was still detectable (D and F). B (left): % of samples with the respective tissue within the fracture gap; B (right): % of samples with bony bridging of the fracture gap. Staining: LL. Single arrow: chondrocytes; dashed arrow: osteocytes. CB, original cortical bone; OC, osseous callus; CA, cartilage; CC, calcified cartilage; IC, immature cartilage; WB, woven bone; F, fracture site; BM, bone marrow; KW, Kirschner wire; AB, air bubble.

easily obtained and reproducible closed fracture healing model.¹² However, the risk of an additional fibular fracture is high (43%,²³). This changes a stable into an unstable fracture model.²⁴ In contrast, the femur is surrounded by a thicker muscle layer, which makes a standardized fracture more difficult. For this reason we detected accordingly to Simon et al. (25.7%,²⁵) an exclusion rate of 24%. Nevertheless, the femur model allows the use of larger implants and

may be preferred when the fracture healing of long bones has to be examined. This standardized widely used fracture model allows results of different studies to be more easily compared.^{26,27} Instead of opening the knee joint for retrograde pinning,²⁸ the K-wire was inserted into the medullary canal of the femur in an antegrade manner.^{18,29} We consider this approach to be less invasive allowing an easier shortening with decreased risk of disability of movement. Because

TABLE III. Biomechanical Parameters

		Mean ± SD	Mean difference (95%-CI)	p values
Breaking load	C	78.54 ± 20.52	C vs K	0.89 (-29.67-31.44)
	K	77.65 ± 41.82		
Stiffness	C	123.74 ± 60.08	C vs K	0.968
	K	122.44 ± 81.16		

Regarding breaking load and stiffness almost identical mean values were generated.

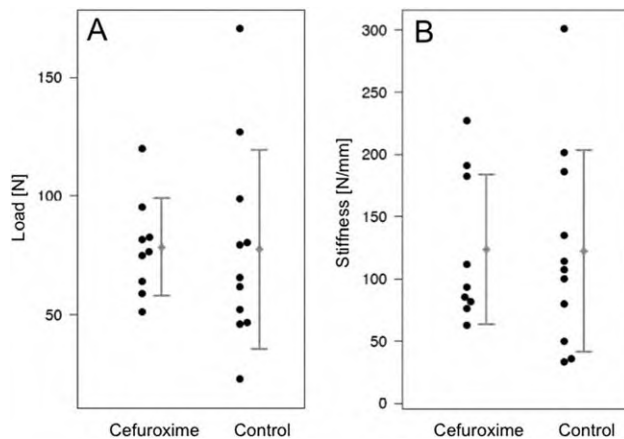


FIGURE 5. Biomechanical parameters as means \pm SD and dotplot of (A) failure load and (B) stiffness. Mean differences and significances are shown in Table III. With respect to the breaking load, the control group revealed a wider spread of the single values in contrast to the cefuroxime group; this influenced the SD (control: 41.82 vs. cefuroxime: 20.52).

of the lack of both axial and rotational stability,²⁷ the K-wire allows micromotion (in contrast to rigid fixation) at the osteotomy site leading to healing by callus formation.²⁹ This is important for the detection of the possible influence of a therapy on healing.³⁰ Freezing after harvesting does not affect the biomechanical properties of the bone adversely³¹. Thus, immediately after thawing, the samples underwent biomechanical examination and were kept moist during the tests.³² However, if the samples are not tested immediately after sacrifice, data from biomechanical tests are relative rather than absolute.³³ Postoperatively, no NSAR or other drugs with a suspected influence on bone metabolism were administered.²⁵

After 21 days, a callus bridging was described for untreated animals—not yet complete and stable,^{34,35} and we expected that, after 21 days, significant differences could be detected, if present. Very early time points are delicate for histological processing and inappropriate for biomechanics,^{27,34} whereas late time points carry the risk that no differences might be detected between the groups because remodelling is too far advanced.^{27,35} However, a possible healing delay within the late phase of fracture healing is not covered by our test approach.^{11,27}

The cefuroxime dose of 30 mg/kg body weight per day to generate human-equivalent pharmacological data was adopted from the literature. Doses for other cephalosporines ranged from 10 to 100 mg/kg of cefazolin^{36–38} or 50 mg/kg of ceftriaxone³⁹ but are comparable with that of cefuroxime. The determined serum levels in our study at 2–3 h after application as trough levels showed that the type and quantity of application of cefuroxime led to values in the therapeutically desired range of 2–20 μ g/mL (Medizinisches Versorgungszentrum Dr. Eberhard & Partner, Dortmund). Since other preliminary studies in rats did not determine the serum concentrations, this fact was of great importance for us in order to obtain more valid results. However, whether an overdose of the human medication is needed at

least in rat models to achieve similar therapeutic results is unknown.

With respect to the μ CT, the cefuroxime group showed similar values to the control group with only marginal differences. Gabet et al. found, by μ CT after 3 weeks, similar callus values to those in our study (about 60 mm³) for their control group when using a closed femur fracture model in rats, a finding that underlines the reproducibility of our results.³⁰ Histological findings were consistent with the radiographic results. Two new surfaces within the periosteal callus were built: an inner layer that had grown over the original cortex and an outer surface that had encapsulated the callus and formed the new interface with the periosteum. Perpendicular to these surfaces in the area of the fracture gap, we found cartilage that had even been replaced by trabecular bone structure in a few cases. The latter and the outer periosteal callus are considered to be responsible for the biomechanical properties.¹⁹ Biomechanically, both in terms of maximum load ($p = 0.95$) and with respect to stiffness ($p = 0.97$), the mean values agreed well with those of the control group. Our results agree well with previous work involving the same animal model. Zhoe et al. generated similar breaking load values of about 75 N after three weeks.⁴⁰ Histologically, a bony fracture gap bridging was shown in the cefuroxime group in 50% of the specimens, which was more frequent than that in the control group (33%), and the ratio bone/cartilage/connective tissue was more favorable. The resorption of the cartilage was pronounced in favor of a more advanced bone healing. Accordingly, in a rabbit study, cefazolin sodium (a first generation cephalosporine) showed a significantly higher histological grading representing the progression of fracture healing compared with the control group. The transition from soft cartilage to calcified cartilage and hard callus was accelerated.³⁶ Another study evaluated a contaminated open fracture model and found that the earlier systemic treatment with cefazolin reduced not only infection, but also the negative impact of delayed surgery.³⁸

In our study, the positive influence on the metabolism of osteoblasts at lower cefuroxime doses, which Salzmann proved *in vitro*, could not significantly be reproduced.⁵ Overall, after 3 weeks, cefuroxime showed no adverse effects on fracture healing compared with the control group, and hence, the inhibiting *in vitro* observations at high concentrations in the animal model could not be confirmed. In particular, this is important with regard to the duration of the application, since the negative effects shown *in vitro* were most pronounced over time. Therefore, cefuroxime may be safely chosen for the treatment of infections in patients with a bone fracture or in bone surgery, because it did not influence bone healing. However, data from animal studies cannot be directly transferred to patients.⁴¹

After the application of antibiotic-impregnated bone cement, antibiotics are released over several weeks: this may additionally result in a prolonged period of action with high concentrations acting on bone cells.^{42,43} Such a setup is not covered by our approach and, thus, care should be taken in the unrestricted usage of impregnated bone cement

as a prophylactic regimen. Further studies should be carried out to examine the release kinetics of cefuroxime-impregnated bone cement and to determine its achievable local concentrations. Additionally, the effects of prolonged high cefuroxime doses on implant incorporation need to be analyzed.

ACKNOWLEDGMENTS

The authors would like to thank Dr. Andres Laib from Scanco Medical (Scanco Medical AG, Brüttisellen, Switzerland) for providing technical support and image analysis and are grateful to thank Professor Karl-Heinz Kunzelmann, Department of Restorative Dentistry, LMU-University, Munich, Germany, for providing the μ Ct 40 and Dr. Eduardo Grande Garcia, Department of Orthopaedic Sports Medicine, Technische Universität München, for the biomechanical support.

REFERENCES

- Einhorn TA, Gerstenfeld LC. Fracture healing: mechanisms and interventions. *Nat Rev Rheumatol* 2015;11:45–54.
- Chen MR, Dragoo JL. The effect of nonsteroidal anti-inflammatory drugs on tissue healing. *Knee Surg Sports Traumatol Arthrosc* 2013;21:540–549.
- Kallala R, Graham SM, Nikkiah D, Kyrkos M, Heliotis M, Mantalaris A, Tsiroidis E. In vitro and in vivo effects of antibiotics on bone cell metabolism and fracture healing. *Expert Opin Drug Saf* 2012;11:15–32.
- Gold B, Rodriguez WJ. Cefuroxime: Mechanisms of action, antimicrobial activity, pharmacokinetics, clinical applications, adverse reactions and therapeutic indications. *Pharmacotherapy* 1983;3:82–100.
- Salzmann GM, Naal FD, von Knoch F, Tuebel J, Gradinger R, Imhoff AB, Schauwecker J. Effects of cefuroxime on human osteoblasts in vitro. *J Biomed Mater Res A* 2007;82:462–468.
- Chiu FY, Chen CM, Lin CF, Lo WH. Cefuroxime-impregnated cement in primary total knee arthroplasty: a prospective, randomized study of three hundred and forty knees. *J Bone Joint Surg Am* 2002;84A:759–762.
- Hughes S, Field CA, Kennedy MR, Dash CH. Cephalosporins in bone cement: Studies in vitro and in vivo. *J Bone Joint Surg Br* 1979;61:96–100.
- Zalavras CG, Patzakis MJ, Holtom P. Local antibiotic therapy in the treatment of open fractures and osteomyelitis. *Clin Orthop Relat Res* 2004;86–93.
- Holtom PD, Pavkovic SA, Bravos PD, Patzakis MJ, Shepherd LE, Frenkel B. Inhibitory effects of the quinolone antibiotics trovafloxacin, ciprofloxacin, and levofloxacin on osteoblastic cells in vitro. *J Orthop Res* 2000;18:721–727.
- Isefuku S, Joyner CJ, Simpson AH. Gentamicin may have an adverse effect on osteogenesis. *J Orthop Trauma* 2003;17:212–216.
- Peric M, Dumic-Cule I, Grcevic D, Matijasic M, Verbanac D, Paul R, Grgurevic L, Trkulja V, Bagi CM, Vukicevic S. The rational use of animal models in the evaluation of novel bone regenerative therapies. *Bone* 2015;70:73–86.
- Bonnarens F, Einhorn TA. Production of a standard closed fracture in laboratory animal bone. *J Orthop Res* 1984;2:97–101.
- Morgan EF, Mason ZD, Chien KB, Pfeiffer AJ, Barnes GL, Einhorn TA, Gerstenfeld LC. Micro-computed tomography assessment of fracture healing: relationships among callus structure, composition, and mechanical function. *Bone* 2009;44:335–44.
- Kazakia GJ, Burghardt AJ, Cheung S, Majumdar S. Assessment of bone tissue mineralization by conventional x-ray microcomputed tomography: Comparison with synchrotron radiation microcomputed tomography and ash measurements. *Med Phys* 2008;35:3170–3179.
- Muller R, Van Campenhout H, Van Damme B, Van Der Perre G, Dequeker J, Hildebrand T, Ruegsegger P. Morphometric analysis of human bone biopsies: A quantitative structural comparison of histological sections and micro-computed tomography. *Bone* 1998;23:59–66.
- Morgan EF, Pittman J, DeGiacomo A, Cushner D, de Bakker CM, Mroszczyk KA, Grinstaff MW, Gerstenfeld LC. BMPRI1A antagonist differentially affects cartilage and bone formation during fracture healing. *J Orthop Res* 2016. doi:10.1002/jor.23233. [Epub ahead of print]
- Burghardt AJ, Kazakia GJ, Laib A, Majumdar S. Quantitative assessment of bone tissue mineralization with polychromatic micro-computed tomography. *Calcif Tissue Int* 2008;83:129–138.
- Huo MH, Troiano NW, Pelker RR, Gundberg CM, Friedlaender GE. The influence of ibuprofen on fracture repair: Biomechanical, biochemical, histologic, and histomorphometric parameters in rats. *J Orthop Res* 1991;9:383–390.
- Krischak GD, Augat P, Sorg T, Blakytyn R, Kinzl L, Claes L, Beck A. Effects of diclofenac on periosteal callus maturation in osteotomy healing in an animal model. *Arch Orthop Trauma Surg* 2007;127:3–9.
- Turner CH, Burr DB. Basic biomechanical measurements of bone: A tutorial. *Bone* 1993;14:595–608.
- Jarvinen TL, Sievanen H, Kannus P, Jarvinen M. Dual-energy X-ray absorptiometry in predicting mechanical characteristics of rat femur. *Bone* 1998;22:551–558.
- Leppanen OV, Sievanen H, Jarvinen TL. Biomechanical testing in experimental bone interventions—May the power be with you. *J Biomech* 2008;41:1623–1631.
- Beck A, Krischak G, Sorg T, Augat P, Farker K, Merkel U, Kinzl L, Claes L. Influence of diclofenac (group of nonsteroidal anti-inflammatory drugs) on fracture healing. *Arch Orthop Trauma Surg* 2003;123:327–332.
- Shefelbine SJ, Augat P, Claes L, Beck A. Intact fibula improves fracture healing in a rat tibia osteotomy model. *J Orthop Res* 2005;23:489–493.
- Simon AM, O'Connor JP. Dose and time-dependent effects of cyclooxygenase-2 inhibition on fracture-healing. *J Bone Joint Surg Am* 2007;89:500–511.
- Reifenrath J, Angrisani N, Lalk M, Besdo S. Replacement, refinement, and reduction: necessity of standardization and computational models for long bone fracture repair in animals. *J Biomed Mater Res A* 2014;102:2884–2900.
- Histing T, Garcia P, Holstein JH, Klein M, Matthys R, Nuetzi R, Steck R, Laschke MW, Wehner T, Bindl R, Recknagel S, Stuermer EK, Vollmar B, Wildemann B, Lienau J, Willie B, Peters A, Ignatius A, Pohlemann T, Claes L, Menger MD. Small animal bone healing models: Standards, tips, and pitfalls results of a consensus meeting. *Bone* 2011;49:591–599.
- Simon AM, Manigrasso MB, O'Connor JP. Cyclo-oxygenase 2 function is essential for bone fracture healing. *J Bone Miner Res* 2002;17:963–976.
- Wingenter S, Calvert G, Tucci M, Tsao A, Russell G, Benghuzzi H. Comparison of two different fixation techniques for a segmental defect in a rat femur model. *J Invest Surg* 2007;20:149–155.
- Gabet Y, Muller R, Regev E, Sela J, Shteyer A, Salisbury K, Chorev M, Bab I. Osteogenic growth peptide modulates fracture callus structural and mechanical properties. *Bone* 2004;35:65–73.
- van Haaren EH, van der Zwaard BC, van der Veen AJ, Heyligers IC, Wuisman PI, Smit TH. Effect of long-term preservation on the mechanical properties of cortical bone in goats. *Acta Orthop* 2008;79:708–716.
- Chu TM, Warden SJ, Turner CH, Stewart RL. Segmental bone regeneration using a load-bearing biodegradable carrier of bone morphogenetic protein-2. *Biomaterials* 2007;28:459–467.
- Burstein AH, Currey JD, Frankel VH, Reilly DT. The ultimate properties of bone tissue: The effects of yielding. *J Biomech* 1972;5:35–44.
- Gerstenfeld LC, Alkhiary YM, Krall EA, Nicholls FH, Stapleton SN, Fitch JL, Bauer M, Kayal R, Graves DT, Jepsen KJ, Einhorn TA. Three-dimensional reconstruction of fracture callus morphogenesis. *J Histochem Cytochem* 2006;54:1215–1228.
- Phillips AM. Overview of the fracture healing cascade. *Injury* 2005;36:S5–S7.
- Akkaya S, Nazali M, Kilic A, Bir F. Cefazolin-sodium has no adverse effect on fracture healing in an experimental rabbit model. *Ekleml Hastalik Cerrahisi* 2012;23:44–48.
- Huddleston PM, Steckelberg JM, Hanssen AD, Rouse MS, Bolander ME, Patel R. Ciprofloxacin inhibition of experimental fracture healing. *J Bone Joint Surg Am* 2000;82:161–173.

38. Penn-Barwell JG, Murray CK, Wenke JC. Early antibiotics and debridement independently reduce infection in an open fracture model. *J Bone Joint Surg Br* 2012;94:107–112.
39. Chen X, Schmidt AH, Tsukayama DT, Bourgeault CA, Lew WD. Recombinant human osteogenic protein-1 induces bone formation in a chronically infected, internally stabilized segmental defect in the rat femur. *J Bone Joint Surg Am* 2006;88:1510–1523.
40. Zhou XZ, Zhang G, Dong QR, Chan CW, Liu CF, Qin L. Low-dose X-irradiation promotes mineralization of fracture callus in a rat model. *Arch Orthop Trauma Surg* 2009;129:125–132.
41. Bigham-Sadegh A, Oryan A. Selection of animal models for pre-clinical strategies in evaluating the fracture healing, bone graft substitutes and bone tissue regeneration and engineering. *Connect Tissue Res* 2015;56:175–194.
42. Xue B, Zhang C, Wang Y, Wang J, Zhang J, Lu M, Li G, Cao Z, Huang Q. A novel controlled-release system for antibacterial enzyme lysostaphin delivery using hydroxyapatite/chitosan composite bone cement. *PLoS One* 2014;9:e113797.
43. Mader JT, Calhoun J, Cobos J. In vitro evaluation of antibiotic diffusion from antibiotic-impregnated biodegradable beads and polymethylmethacrylate beads. *Antimicrob Agents Chemother* 1997;41:415–8.